Study of the Pyrolysis of Biofuels Pellets Blended from Sawdust and Oleic by-Products: A Kinetic Study

Marwa Zribi*, Marzouk Lajili**‡

* UR : EMIR (Etude des Milieux Ionisés et Réactifs), 15 Avenue Ibn eljazzar 5019 Monastir, Tunisie.

**UR: EMIR, Department of physics IPEIM, 15 Avenue Ibn eljazzar 5019 Monastir, Tunisie.

(marwa.zribi01@gmail.com, Marzouk.lajili@ipeim.rnu.tn)

‡ Corresponding Author; Marzouk Lajili, 15 Avenue Ibn Eljazzar IPEIM, Monastir 5019, Tunisie, Tel: +216 73500276

Fax: +216 73500278, Marzouk.lajili@ipeim.rnu.tn

Received: 16.12.2018 Accepted:06.02.2019

Abstract- This work aims to study the slow pyrolysis of agro-pellets produced from olive mill solid waste blended with pine sawdust. Thermogravimetric analyses were conducted under inert atmosphere (N_2) at different heating rates (5°C.min^{-1}, 10°C.min^{-1}, 20°C.min^{-1} and 40°C.min^{-1}) in order to assess the thermal degradation behaviour of the produced agro-pellets. We observed that the different pellets thermal degradations follow the usual behaviour of lignocellulosic materials. Moreover, the kinetic parameters such as the activation energy (E_A) and the pre-exponential factor (A) values were evaluated based on two models. These kinetic parameters are close to those reported in the literature. Hence, the thermo-physical and chemical properties of the produced biofuels promote them as promising alternative fuels for producing energy in domestic or in industrial implementations of heat and or electricity.

Keywords Biomass; pellets; pyrolysis; heating rates; kinetic parameters.

1. Introduction

In shadow of the energy crisis and environmental degradation following the rapid industrialization, the security of energy supply has motivated research in renewable energies worldwide [1, 2, 3]. Moreover, biomass occupies the third place of point of view energy potential rank. This corresponds to about 14% of the world energy consumption with 2900 EJ/y (1EJ = 10^{18}J), especially as this form of renewable and sustainable form of energy can be applied in order to win environmental, technical and economic benefits. The renewability is guaranty by a reasonable forest cutting, residues reuse and by-products valorization. The sustainability can be ensured by respecting the equilibrium of respectively carbon, nitrogen and water cycles.

There are approximately 750 million productive olive trees worldwide, 98% of them are located in the Mediterranean region. The three major olive oil producers worldwide are Spain, Italy, and Greece, followed by Tunisia and Turkey [4]. In Tunisia, the olive wastes produced by the olive oil industry are composed by about 400000 tons of olive pomace per year and about 1000000 t/y of olive mill wastewater [5-8]. However, the woody residues coming from wood manufactories are produced in small amounts. The olive mill solid wastes used in this work are obtained by the three phase's trituration process which is the most used in Tunisia. This lignocellulosic biomass is mainly composed by pulp and pits residues which hold important quantities of organic matter. In addition, about 4% of residual olive oil in the olive mill solid wastes increases the high heating value (HHV) by comparison to the exhausted olive mill solid wastes [7]. Exhausted olive mill solid wastes are obtained when extracting the residual oil from the raw material using an organic solvent (hexane) and a fractioned distillation colon apparatus.

Depending on the temperature and heating conditions, three types of pyrolysis can be distinguished: (1) the slow pyrolysis is carried out with a relatively low heating rate (1-

$10°C.min^{-1}$) [9]. The main product of the slow pyrolysis (carbonization) is the biochar product. It is the so-called charcoal characterized by particle sizing of tens of millimeters). This process takes place at relatively low temperatures (250°C – 600°C). (2) the fast pyrolysis characterized by a more higher heating rate (> $50°Cmin^{-1}$), by a final temperature close to 500°C and with a short residence time in order to avoid the cracking or the recombination of vapors. The resulting degradation reactions give rise to low fractions of charcoal. At the contrary, the condensable vapors (forming the tars) and the biogas are the major components. Rapid cooling of the pyrolysis vapors makes it possible to obtain a liquid commonly called pyrolysis oil or bio-oil. It is to be reminded that this process gives higher yields when working in a fluidized bed. The particle sizes used are in the order of a millimeter [10]. (3) the flash pyrolysis which is realized at very high heating rates conditions reaching few hundreds of degrees/second. Under these conditions, the formation of liquids (tars and oils) is clearly favored. The bio-oil yields can reach 80% [11]. The particles sizes in this case are in the order of hundreds of micrometers [10].

In order to solve the abundant supply of biomass waste generation, the pyrolysis process is selected in this work as an environmental and friendly technic. Indeed, this process provides not only a solution to a pollution source, but also produces a clean renewable energy which can redress the imbalance in the energy balance of an under-developing country like Tunisia. Pyrolysis is a thermal process in an inert atmosphere during which the biomass waste undergoes a thermal degradation using a heat source in a specific temperature range (130°C – 500°C). Indeed, after the dehumidification step the process starts by the release of the volatile matter composed by the bio-oil and the bio-gas, and ends by the charcoal formation. Depending on the used biomass, the heating rate, the residence time and the particle sizing the percentages of the three compounds (biogas, bio-oil and charcoal) will be different [12, 13].

In this study, the used process is the slow pyrolysis based on TGA equipment occurring at relatively low heating rates $5°C.min^{-1}$, $10°C.min^{-1}$, $20°C.min^{-1}$ and $40°C.min^{-1}$ respectively. This protocol is commonly used in industrial applications in the waste treatment domain [14]. The process duration depends on the heating rates. Thus, it can vary from several dozen of minutes to many hours as it takes place at relatively low temperatures. In biomass pyrolysis, thermal degradation behavior results of the degradation of the three main components of biomass; the hemicelluloses, the cellulose and the lignin respectively.

In order to apprehend better the thermal degradation, a kinetic analysis is built based on the diffusion and the chemical reaction mechanisms. This allows us to determine some crucial kinetic parameters involved in the Arrhenius law such as the pre-exponential factor (A), the activation energy (E_a) and the reaction order (n).

2. Materials and Methods

2.1. Samples and preparation:

The raw biomass used in this study is the olive mill solid wastes which were collected from the Zouila oil Press Company situated in Mahdia (the Sahel region of Tunisia). This company is specialized in the second extraction of residual olive oil from olive pomace and in the soap industry. The olive mill solid wastes (OM) are of two types:

- Raw olive mill solid wastes (OM), with initial moisture close to 50-60%.
- Exhausted olive mill solid wastes (EOM), with initial moisture close to 8%.

The pine sawdust (PS) is the second biomass used in this work in order to make the suitable blends was provided from a wood factory situated in the region of Mulhouse in France. Cylindrical pellets of 5-6 mm diameter and 15-30 mm length were prepared as it was mentioned in our previous works [7]. Hence, five pellets types were obtained with different mass fractions of (OM) and PS from 25 to 100% wt of OM:

- OM25PS75: Composed of 25% (OM) and 75% pine sawdust (PS).
- OM50PS50: Composed of 50% (OM) and 50% (PS).
- EOM50PS50: Composed of 50% (EOM) and 50% (PS).
- OM100: Composed of pure unexhausted (OM).
- PS100: Composed of pure pine sawdust.

2.2 Experimental device and kinetic approach

2.2.1. Thermogravimetric analysis:

Thermogravimetric analyses (TGA) were carried out using a KAHN 121 balance. A preliminary blank test should be performed at the beginning to ensure that any trace of oxidizing air is completely discharged from the heat balance, and to avoid any fluctuations by deleting the blank test values from each run values during the data treatment phase. These fluctuations are due to the buoyancy forces caused by the gas flow. This goal can be achieved by circulating a flow of nitrogen (N_2) during 30 min. After this, a sample of 10 mg is introduced, and a rise of temperature under a constant heating rate is performed with a constant gas flow of 12 $NL.h^{-1}$. The thermal degradation will be considered complete when the final temperature of 900°C is reached.

2.2.2. Kinetic approach

The Kinetic study is indispensable for apprehending the course of decomposition-reaction progression and for determining the dependence of the rate of progression on process parameters. Also, the knowledge of the kinetic parameters governing the thermal degradation is essential not only for optimizing the reactors, but also for the prediction of the material lifetime as it was reported by Dhyani et al. [15].

In the literature several approaches based on the kinetic analysis of non-isothermal TGA data were used in order to characterize the decomposition reactions, and to access their kinetic parameters. More precisely, in our study the kinetic parameters were determined using the method based on the

Arrhenius law and which was abundantly reported in literature [16, 17, 18, 19]:

$$K(T) = A \times e^{-\left(\frac{E_a}{RT}\right)} \quad (1)$$

Where, E_a is the activation energy (kJ.mol^{-1}), A is the frequency factor (min^{-1}), R is the universal perfect gas constant (8.314 J. mol^{-1}.k^{-1}) and T is the absolute temperature. The rate of the decomposition reaction in all the kinetic studies is presented by the following expression:

$$\frac{d\alpha}{dt} = K(T) \times f(\alpha) \quad (2)$$

Where α is the degree of conversion of the pyrolysis process, f(α) is a function which depends on the particular decomposition mechanism, K(T) is the decomposition rate function and t is the time.

α is the degree of transformation of the used biomass. It is calculated from the corresponding TG curve using the following formula:

$$\alpha = \frac{w_i - w_t}{w_i - w_f} \quad (3)$$

Where, w_i, w_t, w_t are the initial, at time t and the final mass of the sample respectively.

Since the heating rate is constant, β can be expressed as:

$$\beta = \frac{dT}{dt} = cte \quad (4)$$

The variation of the degree of decomposition can be described as a function of the temperature T:

$$\frac{d\alpha}{dT} = \frac{A}{\beta} exp\left(\frac{-E}{RT}\right) f(\alpha) \quad (5)$$

$$\frac{d\alpha}{f(\alpha)} = \frac{A}{\beta} exp\left(\frac{-E}{RT}\right) dT \quad (6)$$

After the integration of (Eq.6), the following expression can be obtained:

$$g(\alpha) = \int_0^{\alpha} \frac{d\alpha}{f(\alpha)} = \frac{A}{\beta} \int_0^{T} exp\left(\frac{-E}{RT}\right) dT \quad (7)$$

Using the integral method of Coats and Redfern [20], (Eq.7) gives:

$$g(\alpha) = \frac{ART^2}{\beta E}\left(1 - \frac{2RT}{E}\right) exp\left(\frac{-E}{RT}\right) \quad (8)$$

Then, after the division by T^2 and taking logarithms, and assuming that 2RT/E<<1, (Eq.8) gives:

$$Ln\frac{g(\alpha)}{T^2} = Ln\frac{AR}{\beta E} - \frac{E}{RT} \quad (9)$$

Hence, after plotting the linear graph of Ln [g (α)/T^2] as a function of (1/T), a straight line with slope (-E/R) is obtained. Thus, on the basis of the good shape of f(α) and g(α), the activation energy and the frequency factor can be determined from the slope and the intercept of the regression line respectively.

Table 1 lists the functions f(α) and g(α) used in this study to describe the thermal degradation of biomass. Two models were considered based on literature reports for interpreting experimental data resulting from the pyrolysis process [16, 18].

Table 1 Algebraic expressions of the functions reaction mechanisms operating in the reactions in the solid state.

Model	f(α)	g(α)
reaction mechanisms		
F_1	$(1-\alpha)$	$-Ln(1-\alpha)$
F_2	$(1-\alpha)^2$	$[\frac{1}{(1-\alpha)}]^{-1}$
F_3	$(1-\alpha)^3$	$(\frac{1}{2})([1/(1-\alpha)^2]$ (4) $1)$
Diffusion mechanisms		
D_1	$\frac{1}{(2\alpha)}$	α^2 (5)
D2	$[-Ln(1-\alpha)]^{-1}$	$(1-\alpha)Ln(1-\alpha) +$ α (6)
D3	$\frac{3}{2}(1-\alpha)^{2/3}[1$ $-(1-\alpha)^{1/3}]^{-1}$	$[1-(1-\alpha)^{1/3}]^2$
D4	$\frac{3}{2}(1-\alpha)^{1/3}[1$ $-(1-\alpha)^{1/3}]^{-1}$	(7) $\left(1-\frac{2\alpha}{3}\right)$ $-(1-\alpha)^{2/3}$

(8)

3. Results and Discussion

3.1 Thermal degradation under inert atmosphere:

The thermal degradation behavior of the different samples at different heating rates (5, 10, 20, 40°C.min^{-1}) under nitrogen inert atmosphere was examined. **Fig. 1** and **Fig. 2** show the variation of the mass loss (x) and the

opposite of the derivative of the mass loss (-dx/dt) called DTG for the five samples at a heating rate of 5°C.min^{-1}.

As it was reported in literature, the pyrolysis curves follow the usual behavior during the thermal degradation of lingo-cellulosic materials [21]. Indeed, three mass loss steps can be distinguished in the TGA and DTG curves respectively [22]: The first zone of the mass loss is the phase of dehumidification due to the evaporation of the moisture and the loss of light volatiles occurring between 30°C and 170°C. The second zone is the devolatilisation step starting at about 193°C, 183°C, 192°C, 193°C and 218°C respectively for OM25PS75, OM50PS50, EOM50PS50, OM100 and PS100. The fluctuations of initial temperatures of biomass degradation can be attributed to the differences in the elemental and the chemical composition of samples [23]. However, the high mass losses in this region are associated to the decomposition of a part of lignin and especially to holocelluloses (hemicellulose and cellulose). This zone is often called active pyrolysis zone.

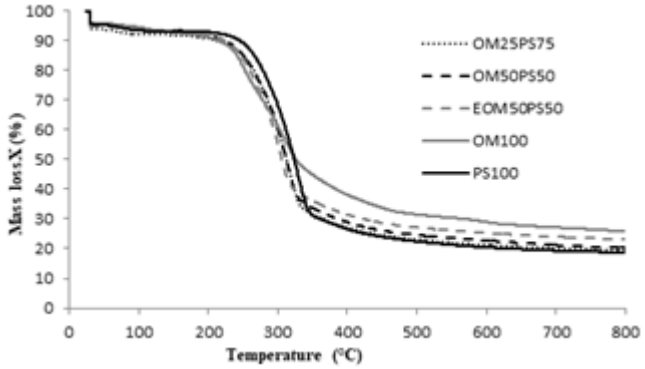

Fig. 1. TGA curves during the thermal degradation of the different samples obtained under inert atmosphere at a heating rate of 5 °C.min^{-1}

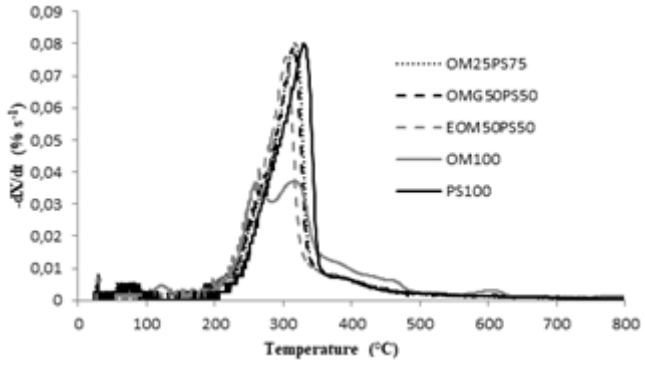

Fig. 2. DTG curves during the thermal degradation of the different samples obtained under inert atmosphere at a heating rate of 5 °C.min^{-1}

Finally, a quite mass loss was observed indicating the decomposition of the not yet degraded lignin. This is the so-called passive pyrolysis which ends when reaching a constant mass composed by the fixed carbon and the ash (constituting all together the charcoal) [24, 25]. According to the analyses of DTG curves, shoulders and peaks are observed in the active pyrolysis zone carried out at different heating rates for all samples (except OM100 for which two peaks; the first on the left is related to the hemicellulose and the other on the right is related to the cellulose) as it is shown on **Fig. 3**. Results obtained at 5°C.min^{-1} is almost the same obtained in our previous work [7]. Moreover, the shoulders are attributed to the hemicelluloses and to a part of lignin decomposition, whereas, the sharp peaks are associated to the cellulose decomposition [26]. At the end of the second step a slow decrease of the mass loss rate is observed. It corresponds to the slow degradation of the not yet degraded lignin. This assumption was already observed for woody biomass [27, 28]. Such thermal behavior may be explained by the difficult decomposition of lignin and its high thermal stability [29,25, 26]. Indeed, it is known that lignin pyrolysis takes place at a temperature ranging between 190°C and 900°C. That's why; we notice the absence of any peak describing the lignin decomposition [30, 31]. Knowing that the cellulose content in the samples (except OM100) is higher than that of hemicellulose (41% against 21% for pomace and 35% against 20% for pine sawdust), it is foreseeable that the intensity of the peak related to cellulose will be higher than that of the shoulder related to hemicellulose. Moreover, the thermal degradation of these samples shows that more the heating rate increases the faster the mass loss will be.

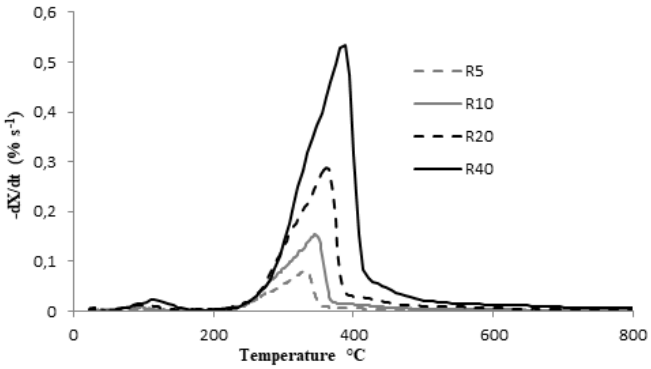

Fig. 3. DTG curves during the thermal degradation of PS100 obtained under inert atmosphere at different heating rate of 5, 10, 20, 40 ° C.min^{-1}

As it is shown on Fig.4, the thermal degradation rates in both active and passive pyrolysis regions increased with the heating rate. This behavior was already reported in the literature for various biomasses [24, 32, 33]. Likewise, it can be seen that when increasing the heating rate, the rate of degradation in the active pyrolysis step is increased significantly. Thus, we concluded that these samples become more reactive when increasing the heating rate from 5°C.min^{-1} to 40°C.min^{-1} as it exhibited in **Fig. 3, Fig. 4, Fig. 5 and Table 2**. Also, we noticed that the heating rate influenced the temperature ranges which encompass all the constituent stages during the pyrolysis process. Indeed, it is clear that the interval temperature corresponding to the active pyrolysis step becomes wider. More precisely, the devolatilisation starts at a lower temperature and ends at a higher one as it is illustrated on **Fig. 3, Fig. 4, Fig. 5,** and in **Table 2**.

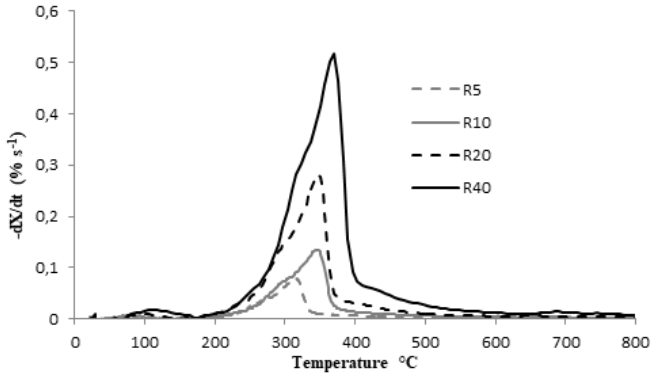

Fig. 4 DTG curves during the thermal degradation of OM50PS50 obtained under inert atmosphere at different heating rate of 5, 10, 20, 40 ° C.min^{-1}

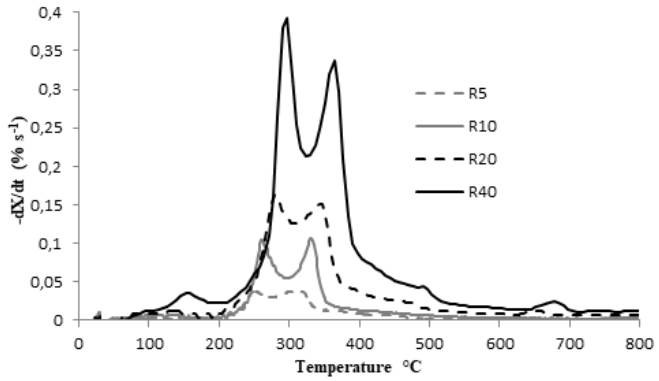

Fig. 5 DTG curves during the thermal degradation of OM100 obtained under inert atmosphere at different heating rate of 5, 10, 20, 40 ° C.min^{-1}

The DTG curves corresponding to the OM100 sample as it was reported in our previous work [7] are characterized by two peaks with almost same intensity corresponding to hemicellulose and cellulose respectively. However, the peaks intensities are highly affected by the imposed heating rates as it is illustrated on **Fig. 5**. More precisely, the peaks intensities increase with the heating rate due to a notable increase of the reactivity. Indeed, the DTG takes its importance from the fact that it constitutes a preliminary indicator of the material reactivity. For a heating rate of 5°C min^{-1}, the maximum rate of mass loss was marked by PS100 and OM25PS75 (approximately 0.08 %.s^{-1}), while the lowest value is obtained for OM100 (approximately 0.038 %.s^{-1}). It is to be mentioned that these obtained results are higher than those found by El May et al. [34], under the same experimental conditions.

Based on previous investigations [35, 36], and using the maximum mass loss R_{peak} and its corresponding temperature T_{peak}, The reactivity can be evaluated using the following expression:

$$R_M = \sum \frac{R_{DTG}}{T_{DTG}} \quad (10)$$

From **Table 2**, and For the heating rate of 5°C.min^{-1}, the R_M values are ranging between 0.14 (for OM100) and 0.25 %.s^{-1}.°C^{-1} (for OM25PS75) respectively. These values are very similar to those reported by El May et al. [35].

3.2 Kinetic analysis:

In order to apprehend the thermo-physical phenomena occurring during the thermal degradation of all samples, we think that it is primordial to determine the kinetic parameters such as the pre-exponential factor A, the activation energy E_a and the order of the reaction. The regression factor R^2 is a crucial control tool for testing the accuracy of our calculations. As it is shown in **Table 3** and in **Table 4**, the performed regression analysis gives correlation coefficients ranging between 85 and 99 % for the different samples. Calculations were carried out in the two main zones corresponding to devolatilisation and to charcoal formation under different heating rates (5, 10, 20 and 40°C.min^{-1}) respectively. For low temperatures, one noticed that the models based on the diffusion mechanism (D_2, D_3, D_4) lead to the best fits with the experimental data. More precisely, this is the D_3 mechanism which gives the best correlation (i.e. the highest regression factor). This result is in a perfect agreement with what was reported in the literature [34, 37-39]. The obtained analysis of the kinetic parameters show that for a given heating rate, the highest values of the activation energy during the active pyrolysis phase (devolatilisation step) were obtained with the PS100 sample, while the lowest values were obtained with the OM100 sample. This is the major interest of olive wastes biofuels which are known by their character to be highly flammable. However, the highest frequency factor corresponds to PS100 sample. This crucial parameter playing an important role in the reactivity of thermal degradation can be considered as an advantage for the blended samples **(Table 3)**. Our obtained results are found to be quietly higher than those found by Chouchene et al. [40].

For high temperatures (i.e. the charcoal formation zone), the models based on the chemical reaction mechanism are dominants. More precisely, the third order chemical reaction mechanism (F_3) gives the best correlation for all samples in agreement with some results reported in the literature [34, 39]. Indeed, it was found that during the char formation the highest activation energy was obtained with the OM100 sample, followed by PS100, EOM50PS50, OM50PS50 and OM25PS75 respectively. This fact can be explained by the high molecular weight of components constituting the lignin of the OM100 sample. Indeed, raw olive residues are known to be rich in fiber (crude cellulose and ADF). Furthermore, the degradation of these components is hard which can be explained by their relatively high activation energy. Hence, the activation energy values during this step can be related to the fixed carbon and the ash contents as it was stated by Chaabane et al. [41]. It is to be mentioned that the obtained values of the activation energy we found in this work are higher than those reported in some works in the literature [26, 31]. In addition, the variation of the activation energy for the different samples proves that the chemical reaction regimes are governing the thermal degradation of the different samples [42]. Furthermore, the highest activation energies (in the range of 79.20 and 119.98 kJ.mol^{-1}) were found in the first zone (active pyrolysis) where the main pyrolysis reaction took place and the largest weight loss occurred [43].

In the same context we concluded that the activation energy values we found are higher than those obtained during a fast pyrolysis process [44]. This can be explained by the fact that the residence time is longer during the slow pyrolysis. Other reasons that may cause much lower values of activation energy during the fast pyrolysis may be related to the much higher heating rates and to more catalysts effect efficiency.

Table 2 Characteristics of pyrolysis under inert atmosphere.

	temperature ranges (°C)	$R_{shoulder}$ (% s^{-1})	$T_{shoulder}$ (°C)	R_{peak} (% s^{-1})	T_{peak} (°C)	$R_M \times 10^3$ (% s^{-1} C^{-1})
PS100 :						
R5	218-576	0.04	282	0.08	332	0.24
R10	220-612	0.08	296	0.15	346	0.43
R20	234-671	0.14	304	0.29	361	0.80
R40	234-749	0.38	348	0.54	381	1.41
OM25PS75 :						
R5	193-569	0.04	274	0.08	317	0.25
R10	182-576	0.07	284	0.15	331	0.45
R20	202-596	0.15	302	0.28	352	0.79
R40	214-641	0.31	327	0.54	374	1.44
OM50PS50 :						
R5	183-682	0.04	274	0.07	315	0.22
R10	186-706	0.08	310	0.13	346	0.38
R20	183-744	0.17	310	0.28	347	0.81
R40	203-764	0.32	323	0.52	370	1.40
EOM50PS50 :						
R5	192-621	0.04	262	0.07	304	0.23
R10	180-667	0.08	272	0.15	317	0.47
R20	194-778	0.16	298	0.27	338	0.80
R40	211-719	0.34	311	0.56	351	1.60
OM100 :						
	temperature ranges (°C)	R_{peak1} (% s^{-1})	T_{peak1} (°C)	R_{peak2} (% s^{-1})	T_{peak2} (°C)	$R_M \times 10^3$ (% s^{-1} C^{-1})
R5	193-696	0.04	252	0.04	319	0.14
R10	207-746	0.10	262	0.11	332	0.35

R20	210-764	0.16	280	0.15	343	0.50
R40	218-765	0.36	297	0.34	364	0.65

Table 3 Kinetic parameters during the step of the devolatilization under an inert atmosphere for different heating rates: 5, 10, 20, 40 ° C.min^{-1}

Sample	Heating rate (°C min^{-1})	Temperature range (°C)	n	E_a (kJ mol$^{-1)}$	A(s^{-1})	R^2	f(α)
PS100	5	222-358	0.695	98.95	2.26×10^5	0.857	D2
				116.29	2.87×10^6	0.919	D3
				104.91	2.01×10^5	0.833	D4
	10	216-374	0.58	103.03	6.34×10^5	0.898	D2
				118.07	4.73×10^6	0.943	D3
				108.19	4.70×10^5	0.916	D4
	20	224-391	0.56	104.44	9.95×10^5	0.898	D2
				119.98	6.78×10^6	0.943	D3
				109.57	7.15×10^5	0.917	D4
	40	215-421	0.52	103.97	8.06×10^5	0.918	D2
				117.13	3.69×10^6	0.954	D3
				108.51	5.09×10^5	0.933	D4
OM25PS75	5	204-346	0.63	91.01	6.3×10^4	0.884	D2
				105.32	4.47×10^5	0.931	D3
				95.92	4.62×10^4	0.904	D4
	10	187-357	0.63	89.68	6.75×10^4	0.939	D2
				100.45	2.15×10^5	0.959	D3
				93.37	3.74×10^4	0.948	D4
	20	176-382	0.54	84.77	2.48×10^4	0.941	D2
				93.91 87.90	5.36×10^4	0.957	D3 D4
					1.2×10^4	0.948	
	40	181-407	0.47	86.42			D2
				95.51	3.70×10^4	0.946	D3
				89.54	7.54×10^4	0.961	D4
					1.76×10^4	0.953	
OM50PS50	5	195-344	0.71	87.55	3.10×10^4	0.899	D2

				100.00	14.58×10^4	0.937	D3
				91.80	1.97×10^4	0.915	D4
	10	190-380	0.67	82.38	7.96×10^3	0.921	D2
				92.35	2.01×10^4	0.948	D3
				85.80	4.06×10^3	0.932	D4
	20	181-377	0.46	83.35	2.19×10^4	0.939	D2
				93.09	5.42×10^4	0.960	D3
				86.68	1.11×10^4	0.948	D4
	40	177-403	0.43	84.49 93.33	2.80×10^4	0.943	D2
				87.52	5.47×10^4	0.961	D3
					1.31×10^4	0.951	D4
EOM50PS50	5	210-339	0.65	96.38	8.08×10^4	0.875	D3
				86.17	6.92×10^3	0.828	D4
	10	194-347	0.65	103.38	5.13×10^6	0.939	D3
				95.55	7.44×10^5	0.918	D4
	20	194-368	0.65	104.19	6.22×10^5	0.945	D3
				96.88	1.06×10^4	0.926	D4
	40	185-424	0.58	88.06	1.55×10^4	0.887	D3
				80.37	2.41×10^3	0.850	D4
OM100	5	179-346	1.13	70.89	7.68×10^2	0.901	D2
				79.20	1.43×10^3	0.935	D3
				73.72	3.52×10^2	0.914	D4
	10	210-360	1.34	121.30	2.29×10^5	0.766	D2
				87.78	1.31×10^4	0.846	D3
				79.71	1.88×10^3	0.803	D4
	20	203-380	1.21	72.23	1.85×10^3	0.855	D2
				81.92	4.28×10^3	0.903	D3
				75.53	9.11×10^2	0.874	D4
	40	218-397	1.17	71.999	2.58×10^3	0.832	D2
				83.11	7.86×10^3	0.888	D3
				75.79	1.40×10^3	0.854	D4

Table 4 Kinetic parameters during the step of the char formation under an inert atmosphere for different heating rates: 5, 10, 20, 40 ° C.min^{-1}

Sample	Heating rate (°C min^{-1})	Temperature range (°C)	E (kJ mol^{-1})	A (s^{-1})	R^2	f(α)
PS100	5	358-462	44.45	154.16	0.935	F3
	10	374-483	40.58	134.69	0.935	F3
	20	391-511	33.75	63.50	0.961	F3
	40	421-528	26.84	45.60	0.949	F3
OM25PS75	5	366-478	32.90	18.45	0.918	F3
	10	357-511	37.84	75.79	0.980	F3
	20	382-523	37.58	126.22	0.969	F3
	40	407-547	32.66	93.97	0.968	F3
OM50PS50	5	344-479	36.98	27.22	0.939	F3
	10	380-561	29.11	6.23	0.985	F3
	20	377-551	35.83	85.88	0.979	F3
	40	403-584	32.08	64.91	0.974	F3
EOM50PS50	5	339-464	40.35	47.18	0.968	F3
	10	347-497	37.45	5.03×10^2	0.981	F3
	20	368-528	36.32	70.60	0.979	F3
	40	424-551	31.52	57.11	0.981	F3
OM100	5	346-429	48.06	86.40	0.977	F3
	10	360-485	36.85	19.63	0.984	F3
	20	380-493	35.73	20.21	0.963	F3
	40	397-471	40.51	120.30	0.987	F3

4. Conclusion

In this study, slow pyrolysis tests of 5 pellets types prepared from olive mill solid wastes (OM) and pine sawdust (PS) at different heating rates were carried out. Obtained results show three steps forming the whole process of a lignocellulosic biomass material; the dehumidification, the devolatilisation and the charcoal formation.

When working at different heating rates, it is possible to apprehend the reactivity mechanisms and the spreading of the temperature range during which the conversion occurs. A detailed kinetic study based on the Arrhenius, allowed us to assess the most crucial parameters governing the pyrolysis process for all samples. We conclude that the devolatilisation zone is governed by the diffusion mechanisms, whereas the charcoal formation zone is governed by chemical reaction mechanisms. Furthermore, it was found that the kinetic parameters depend not only on the pyrolysis type process, but also on the composition of the biomass. Moreover, the activation energy and the frequency factor are found higher during the devolatilisation phase than during the char formation step.

Acknowledgments

Marzouk lajili would like to express deep thinks to the director of GRE laboratory of Mulhouse (France) and

especially, to Damaris Kehrli for hosting him and for all their technical assistance.

References

[1] W. Anggono, Sutrisno, F.D. Suprianto, J. Evander, G.J. Gotama, "Biomass Briquette Investigation from Pterocarpus Indicus Twigs Waste as an Alternative Renewable Energy", Int. J. Renew. Energy. Res, vol. 8, No.3,2018.

[2] H.C. Teng, B.C. Kok, C. Uttraphan, M.H. Yee, "A Review on Energy Harvesting Potential from Living Plants: Future Energy Resource", Int. J. Renew. Energy. Res, vol. 8, No.4, 2018.

[3] J. Morel, S. Obara, K. Sato, D. Mikawa, H. Watanabe, T. Tanaka, "Contribution of a Hydrogen Storage-TransportationSystem to the Frequency Regulation of a Microgrid", 4th International Conference on Renewable Energy Research and Applications, Palermo, 22-25 Novemeber 2015.

[4] E. Tsagaraki, H.N. Lazarides, K.B. Petrotos, Utilization of By-Products and Treatment of Waste in the Food Industry. New York: Springer, 2017, Ch. 4.

[5] V.K. Verma, S. Barm, F. Delattin, P. Laha, I. Vandendeal, A. Hubin, et al, "Agropellets for domestic heating boiliers: standard laboratory and real life performance", Appl. Energy, vol. 90, pp. 17-23, 2012.

[6] T. Miranda, J.I. Arranz, I. Montero, S. Roman, C.V. Rojas, S. Nogales, "Characterization and combustion of olive pomace and forest residue pellets", Fuel. Process. Technol, vol. 103, pp. 91-96, 2012.

[7] M. Lajili, L. Limousy, M. Jeguirim, "Physico-chemical properties and thermal degradation characteristics of agro pellets from olive mill by-products/sawdust blends", Fuel. Process. Technol, vol. 126, pp. 215-221, 2014

[8] R. S'habou, M. Zairi, A. Kallel, A. Aydi, H. Ben Dhia, "Assesing the effect of an olive mill wastewater evaporation pond in Sousse, Tunisia", Environ. geol, vol. 58, pp. 679-686, 2008.

[9] F. Collard, New catalytic strategies for biomass gasification: influence of impregnated metals on pyrolis mechanisms, International Institute for Water and Environmental Engineering, 2012.

[10] M.J. Ngollo, Study of the carbonization-pyrolysis of eucalyptus wood by thermogravimetric method, International Institute for Water and Environmental Engineering, 2010.

[11] K. Raveendran, A. Ganesh, K.C. Khilar, "Pyrolysis charecteristics of biomass and biomass components", Fuel, vol. 75, pp. 987-998, 1996.

[12] O. Onay, "Influence of pyrolysis temperature and heating rate on the production of bio-oil and char from safflower seed by pyrolysis, using a well-swept fixed-bed reactor", Fuel. Process. Technol, vol. 88, pp. 523-531, 2007.

[13] J. Kandasamy, I. Gokalp, "Pyrolysis, combustion, and steam gasification of various types of scrap tires for energy", Energy. Fuels, vol. 19, pp. 346-354, 2015.

[14] M. Ryms, K. Januszewicz , W.M. Lewandowski, E. Klugmann-Radziemska, "Pyrolysis process of whole waste tires as a biomass energy recycling", Versita, vol. 20, pp. 93-107, 2013.

[15] V. Dhyani, T. Bhaskar, "A comprehensive review on the pyrolysis of lignocellulosic biomass", Renew. Energy, vol. 129, pp. 695-716, 2017.

[16] M. Jeguirim, Y. Elmay, L. Limosy, M. Lajili, R. Said, "Devolatilization behavior andpyrolysis kinetics of potential Tunisian biomass fuels", Environ. Prog. Sustain. Energy, vol. 33, pp. 1452-1458, 2014.

[17] A. Kumar, L. Wang, Y. Dzenis, D.D. Jones, M.A. Hanna, "Thermogravimetric characterization of corn Stover as gasification and pyrolysis feedstock", Biomass. Bioenergy, vol. 32, pp. 460–467,2008.

[18] M. Jeguirim, S. Dorge, A. Loth, G. Trouvé, "Devolatilization kinetics of miscanthus straw from thermgravimetric analysis", Int. J. Green. Energy, vol. 7, pp. 164-173, 2010.

[19] Brown , M. Ewart, Introduction to thermal analysis, Techniques and applications, 2nd ed., vol. 1. Netherlands: Springer, 2001.

[20] A.W. Coats, J.P. Redfern, "Kinetic parameters from thermogravimetric data.II", J. Polym. Sci., Part B: Polym. Phys, vol. 3, pp. 917–920, 1965.

[21] J.J.M. Órfão, F.J.A. Antunes, J.L. Figueiredo, "Pyrolysis kinetics of lignocellulosic materials three independent reactions model", Fuel, vol. 78, pp. 349-358,1999.

[22] I. Obernberger, T. Brunner, G. Barnthaler, "Chemical properties of solid biofuels significance and impact", Biomass. Bionergy, vol. 30, pp. 973-982, 2003.

[23] K.G. Mansaray, A.E. Ghaly, "Thermal degradation of rice husks in nitrogen", Bioresour. Technol, vol. 65, pp. 13-20, 1998.

[24] M. Jeguirim, G. Trouvé, "Pyrolysis characteristics and kinetics of Arundodonax using thermogravimetric analysis", Bioresour. Technol, vol. 100, pp. 4026–403, 2009.

[25] Y. Haiping, Y. Rong, C. Hanping, Z. Chuguang, L. Dong Ho, L. David Tee, "In depth investigation of biomass pyrolysis based on three major components: Hemicellulose, Cellulose and Lignin", Energy. Fuels, vol. 20, pp. 388–393, 2006.

[26] Y. Fei, W. Qinglin, L. Yong, G. Weihong, X. Yanjun, "Thermal decomposition kinetics of natural fibers: Activation energy with dynamic thermogravimetric analysis", Polym. Degrad. Stab, vol. 93, pp. 90–98, 2008.

[27] Y. Wei, I. Schintia, J.C. Coronella, V.R. Vásquez, "Pyrolysis kinetics of raw/hydrothermally carbonized lignocellulosic biomass", Environ. Prog. Sustain. Energy, vol. 31, pp. 200-204, 2012.

[28] P. Ghetti, L. Ricca, L. Angelini, "Thermal analysis of biomass and corresponding pyrolysis products", Fuel, vol. 75, pp. 565–573, 1996.

[29] M. Alhinai, A.K. Azad, M.S. Abu Bakar, N. Phusunti, "Characterisation and Thermochemical Conversion of Rice Husk for Biochar Production", Int. J. Renew. Energy. Res, vol. 8, No.3,2018.

[30] I. Abed, M. Paraschiv, K. Loubar, F. Zagrouba, M. Tazerout, "Thermogravimetric investigation and thermal conversion kinetics of typical North-Africa and middle-east lignocellulosic wastes", BioResources, vol. 7, pp. 1200–1220, 2012.

[31] S. Li, S. Xu, S. Liu, C. Yang, Q. Lu, "Fast pyrolysis of biomass in free fall reactor for hydrogen-richgas", Fuel. Process. Technol, vol. 85, pp. 1201-1211, 2004.

[32] C.A. Koufopanos, G. Maschio, A. Lucchesi, "Kinetic modelling of the pyrolysis of biomass and biomass components", Can. J. Chem. Eng, vol. 67, pp. 75-84, 1989.

[33] A.E. Ghaly, K.G. Mansaray, "Comparative study of the thermal degradation of rice husks in various atmospheres", Energy. Sourc, vol. 21, pp. 867-882, 1999.

[34] Y. Elmay, M. Jeguirim, S. Dorge, G. Trouvé, R. Said, "Thermogravimetric analysis and kinetic study on palm of phoenix dactylifera L", 7th Mediterranean Combustion Symposium, Italy: Chia Laguna, 11-15 Sept 2011.

[35] Y. Elmay, M. Jeguirim, S. Dorge, G. Trouvé, R. Said, "Study on the thermal behavior of different date palm residues: characterization and devolatilization kinetics under inert and oxidative atmospheres", Energy, vol. 44, pp. 702–709, 2012.

[36] S. Munir, S.S. Daood, W. Nimmo, A.M. Cunliffe, B.M Gibbs, "Thermal analysis and devolatilization kinetics of cotton stalk, sugar cane bagasse and shea meal under nitrogen and air atmospheres", Bioresour. Technol, vol. 100, pp. 14143-1418, 2009.

[37] R.K. Agarwal, "On the use of the Arrhenius equation to describe cellulose and wood pyrolysis", Thermochim. Acta, vol. 91, pp. 343–349, 1985.

[38] J. Guo, A.C. Lua, "Effect of heating temperature on the properties of chars and activated carbons prepared from oil palm stones", J. Therm. Anal. Calorim, vol. 60, pp. 417–425, 2000.

[39] Y. Wu, D. Dollimore, "Kinetic studies of thermal degradation of natural cellulosic materials", Thermochim. Acta, vol. 324, pp. 49–57, 1998.

[40] A. Chouchene, M. Jeguirim, A. Favre Reguillon, G. Trouvé, G. Le Buzit, B. Khiari, et al, "Energetic valorisation of olive mill wastewater impregnated on low cost absorbent: Sawdust versus olive solid waste", Energy, vol. 39, pp. 74-81, 2012.

[41] K. Chaabane, R. Bergaoui, M. BenHammoda, "Utilisation de differents types de grignons d'olive dans l'alimentation des lapereaux", World-Rabbit. Sci. J, vol. 5, pp. 17-21, 1997.

[42] H.H. Sait, A. Hussain, A.A. Salema, F.N. Ani, "Pyrolysis and combustion kinetics of date palm biomass using thermogravimetric analysis", Bioresour. Technol, vol. 118, pp. 382–389, 2012.

[43] Y. Elmay, M. Jeguirim, G. Trouvé, R. Said, "Kinetic analysis of thermal decomposition of date palm residues using Coats–Redfern method", Energy. sourc, vol. 38, pp. 1117-1124, 2016.

[44] A.A. Zabaniotou, G. Kalogiannis, E. Kappas, A.J. Karabelas, "Olive residues (cuttings and kernels) rapid pyrolysis product yields and kinetics", Biomass. Bioenergy, vol. 18, pp. 411-420, 2000.